




## CLINICAL ARTICLE

# Micro-Computed Tomography Analysis of Femoral Head Necrosis After Long-Term Internal Fixation for Femoral Neck Fracture

Yang Liu, MM<sup>1,2</sup> , Haoran Liang, MM<sup>1,2†</sup>, Xin Zhou, MM<sup>1,2</sup>, Wenjie Song, MM<sup>1,2</sup>, Huifeng Shao, EngD<sup>3,4,5</sup>, Yong He, EngD<sup>4,5</sup>, Yanfei Yang, MM<sup>1,2</sup>, Li Guo, MD<sup>1,2</sup>, Pengcui Li, MD<sup>1,2</sup>, Xiaochun Wei, MD<sup>1,2</sup> , Wangping Duan, MD<sup>1,2</sup> 

<sup>1</sup>Department of Orthopaedics, Second Hospital of Shanxi Medical University and <sup>2</sup>Shanxi Key Laboratory of Bone and Soft Tissue Injury Repair, Taiyuan and <sup>3</sup>School of Mechanical Engineering, Hangzhou Dianzi University and <sup>4</sup>State Key Laboratory of Fluid Power and Mechatronic Systems and <sup>5</sup>Key Laboratory of 3D Printing Process and Equipment of Zhejiang Province, School of Mechanical Engineering, Zhejiang University, Hangzhou, China

**Objective:** To analyze necrotic femoral head after long-term internal fixation for femoral neck fractures using micro-computed tomography (CT) for bone histomorphometry.

**Methods:** The experimental group included six patients (two men and four women; mean age  $62.00 \pm 9.36$  years) who underwent hip arthroplasty at  $47.67 \pm 14.22$  months after internal fixation. Surgery was performed because of femoral head necrosis after femoral neck fracture between October 2018 and October 2020. The control group included three patients (two men and one woman; mean age  $69.33 \pm 4.62$  years) who underwent hip arthroplasty for femoral neck fracture. In the experimental group, micro-CT quantitative analysis of the whole femur, sclerotic region around screws, screw paths, sclerotic region and screw paths, and relatively normal region was performed. The bone volume fraction (BV/TV), number of bone trabeculae (Tb.N), connection density (Conn.D), thickness of bone trabeculae (Tb.Th), separation of bone trabeculae (Tb.SP), structural model index (SMI), and bone mineral density (BMD) of each part were quantitatively analyzed.

**Results:** The BV/TV ( $0.3180 \pm 0.0617$ ), Conn.D ( $6.9261 \pm 2.4715/\text{mm}^3$ ), Tb.Th ( $0.3262 \pm 0.0136 \mu\text{m}$ ), and BMD ( $298.9241 \pm 54.2029 \text{ g/cm}^3$ ) of the sclerotic region around the screws were significantly higher in the experimental group than the BV/TV ( $0.1248 \pm 0.0390$ ), Conn.D ( $2.5708 \pm 0.5187/\text{mm}^3$ ), Tb.Th ( $0.1713 \pm 0.0333 \mu\text{m}$ ), and BMD ( $66.5181 \pm 43.0380 \text{ g/cm}^3$ ) in the control group ( $P < 0.05$ ). The BV/TV ( $0.2222 \pm 0.0684$ ), Tb.Th ( $0.2775 \pm 0.0326 \mu\text{m}$ ), and BMD ( $195.0153 \pm 71.8509 \text{ g/cm}^3$ ) in the collapsed region were significantly higher in the experimental group than in the control group ( $P < 0.05$ ). In the experimental group, the volume ratio of the sclerotic region around screws and screw paths to the entire femoral head was  $0.4964 \pm 0.0950$ .

**Conclusion:** After internal fixation for femoral neck fracture, a large number of sclerotic plate-like trabeculae were observed around the long-term retained implant. The screw paths and surrounding sclerotic comprise approximately 50% of the femoral head volume.

**Key words:** Femoral neck fracture; Femur head; Microcomputed tomography; Necrosis; Three-dimensional imaging

## Introduction

With the rapid development of modern industry, construction, and transportation, there is a trend of

increasing incidence of hip fractures among younger individuals caused by high-energy injuries.<sup>1</sup> Femoral neck fractures account for approximately 3.58% of total body fractures.<sup>2</sup>

**Address for correspondence** Wangping Duan, MD, Department of Orthopaedics, Second Hospital of Shanxi Medical University, No. 382, Wuyi Road, Taiyuan, Shanxi, China 030001 Tel: 0086-351-3365646; Email: [dwpssc2004121@163.com](mailto:dwpssc2004121@163.com)

<sup>†</sup>Haoran Liang's contribution is equal to the first author.

Received 3 September 2021; accepted 21 April 2022

Artificial hip replacement can be used as a treatment option for femoral neck fractures in older patients aged >65 years. However, young and middle-aged patients with femoral neck fractures are mainly treated with closed reduction and internal fixation with cannulated screws.<sup>3</sup> The importance of early surgery and accurate anatomical reduction should be highlighted in young and middle-aged patients with femoral neck fractures to minimize local blood supply disruption and early restoration of the blood circulation of the femoral head.<sup>4,5</sup> With the development of imaging and internal fixation techniques, the fracture healing rate after internal fixation of femoral neck fractures with cannulated screws has reached over 90%.<sup>1,6</sup> However, some studies have indicated that the rate of femoral head necrosis after internal fixation for femoral neck fracture in middle age remains as high as 40%–80%,<sup>7,8</sup> and femoral head collapse has been reported in 70%–80% of cases within 1–3 years of necrosis.<sup>9</sup> The management of femoral neck fracture in middle age remains controversial.

Mechanical analysis indicated that after internal fixation for femoral neck fracture with cannulated screws, the mechanical loads are concentrated on the internal fixation material, which alters the bone mass and microstructure of the femoral head.<sup>10–12</sup> After long-term retention of the internal fixation implant following surgery for femoral neck fracture, computed tomography revealed apparent sclerosis around the screw paths of the femoral head (Fig. 1). Additionally, there was no obvious regeneration tissue filling in the screw path in the femoral head for approximately 1 year after the removal of long-term retained internal fixation. This further reduces the osteogenic vascularization and mechanical properties of the entire femoral head, accelerating necrosis of the femoral head. In the later stage, despite the removal of internal fixation after long-term retention, effective filling and the recovery of blood supply could not occur owing to a lack of osteogenic vascularization around the screw path. This may be the mechanism underlying the acceleration of the femoral head necrosis due to the extended

retention of the internal fixation. An analysis of the effects of internal fixation after femoral neck fracture, particularly the influence of the long-term retention of implants on the histological structure of the femoral head, can help to further clarify the mechanisms underlying femoral head necrosis after femoral neck fracture surgery and the optimal removal timing of the internal fixation postoperatively in the clinical setting.<sup>13</sup>

The aim of this study was to analyze femoral head necrosis after internal fixation for femoral neck fractures in middle age using micro-CT bone morphometric analysis. In addition, considering that the femoral head remains necrotic despite a well-healed femoral neck fracture, we discussed the relationship between long-term internal fixation and femoral head necrosis. We hypothesized that the long-term retention of internal fixation after femoral neck fracture leads to tissue sclerosis around the screw paths and osteogenic vascularization obstacles.

## Methods

### Acquisition and Storage of Samples

Six patients (two men and four women), with an average age of  $62.00 \pm 9.36$  years, who underwent hip replacement surgery at the Second Hospital of Shanxi Medical University for femoral head necrosis after femoral neck fracture surgery between October 2018 and October 2020, were selected. The mean time from internal fixation for femoral neck fracture to hip replacement for femoral head necrosis was  $47.67 \pm 14.22$  months. Three patients (two men and one woman) with a mean age of  $69.33 \pm 4.62$  years, who underwent hip replacement for femoral neck fracture during the same period, were selected as healthy controls.

### Inclusion and Exclusion Criteria

Femoral neck fracture: patients with simple Garden II, III and IV femoral neck fractures or those aged >60 years were included, and patients with congenital hip dysplasia, femoral

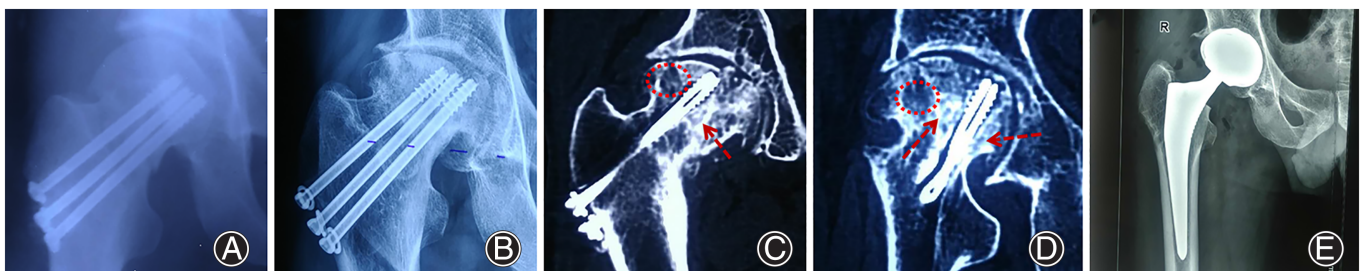


**Fig. 1** Imaging analysis of a typical case of postoperative femoral neck fracture in a middle-aged patient. The patient was a 54-year-old man with a right femoral neck fracture caused by a fall in 2008. (A) Anteroposterior radiograph of the hip joint after internal fixation with cannulated screws. (B) The patient developed pain in the affected hip in 2014, which gradually worsened and limited movement in 2017, and femoral head necrosis of the hip joint was detected on review of the radiograph. (C, D) A computed tomography scan of the hip joint during hospitalization on December 22, 2017 indicated the formation of a mass of sclerotic bone around the screw paths (shown by red arrows) secondary to a large number of surrounding necrotic cavities (shown by red circles) and collapse of the femoral head. (E) Total hip arthroplasty was performed for treatment.

head deformities, bone tumors, and a history of internal fixation of the femoral head were excluded. Femoral head necrosis after femoral neck fracture surgery: middle-aged patients (age < 65 years) with a history of internal fixation for femoral neck fracture<sup>14</sup> whose fractures had healed were included, excluding patients with pathological fractures, those taking hormones during internal fixation, or patients with a history of re-trauma. After obtaining the patient's informed consent and approval from the Ethics Committee of the Second Hospital of Shanxi Medical University, all femoral head specimens were preserved at the time of joint replacement surgery, and general data including the patient's name, age, sex, hospitalization number, medical history, and relevant imaging data such as radiographs, CT, and magnetic resonance imaging, were retained at the same time. A typical case is shown in Fig. 1.

To ensure the integrity of the femoral head specimen and avoid intraoperative damage to the femoral head tissue, a head extractor (artificial hip surgical auxiliary tool) was applied. After the removal of the intraoperative femoral head, the specimen was immediately placed in a specimen bag and marked with basic information, including the patient's name, age, and date of surgery. The specimen was then placed in an ice box and transferred to the laboratory for storage in a refrigerator at  $-80^{\circ}\text{C}$ .

## Experimental Methods

### Micro-CT Analysis

All specimens were measured using the microstage in a plastic tube of the Micro-CT system ( $\mu\text{CT-80}$ , Scanco Medic, Bassersdorf, Switzerland) with the following scanning parameters: source current of  $113\ \mu\text{A}$  and source voltage of  $70\ \text{kV}$ . Continuous scanning was performed from the anterior to posterior side along the coronal plane of the femoral neck and femoral head in the direction of cannulated screw placement, and successive micro-CT two-dimensional (2D) images were acquired with a flat image resolution of  $1024 \times 1024$ , pixel size of  $20\ \mu\text{m} \times 20\ \mu\text{m}$ , and layer spacing of  $20\ \mu\text{m}$  (Fig. 2A). Compared with the histomorphology of the femoral head specimen after normal femoral neck fracture, the femoral head specimen after internal fixation treatment for femoral neck fracture was divided into three regions: sclerotic region, collapsed region, and relatively normal region (Fig. 2B). To investigate the effect of implants on the surrounding femur, the entire femoral head specimen and region of interest were selected separately (sclerotic region around the screws, collapsed region, and relatively normal region). In addition, 2D tomographic images showing the region of interest on the N-layer were selected and reconstructed. These were used to obtain bone trabecular parameters and 2D and 3D images of the entire femoral head with each region of interest (Fig. 3).

### Metrological Analysis of 3D Parameters

The selected 2D images were analyzed and reconstructed using Scanco software (SCANCO Medical AG, Wangen-Brüttisellen, Switzerland). Bone histometric parameters included<sup>15</sup>: (i) the bone volume fraction (BV/TV) (%), which reflects the value of bone volume and serves as a significant index for evaluating the alteration of bone mass; (ii) the trabecular number (Tb.N) (1/mm), which is the number of intersections between bone tissue and non-bone tissue within a given length. This index can reflect the morphological structure of bone trabeculae and the ratio of bone area to bone mass, explaining the change in bone mass. For a certain width of bone trabeculae, the greater the number of trabeculae, the greater the bone mass; (iii) the connectivity density (Conn.D.) ( $\text{n}/\text{mm}^3$ ), which is the degree of interconnection between bone trabecular structures, indicating the quantity of connection in the trabecular meshwork per cubic millimeter; (iv) The trabecular thickness (Tb.Th) ( $\mu\text{m}$ ), which is the average thickness of bone trabeculae; (v) The trabecular separation (Tb.Sp) ( $\mu\text{m}$ ), which is the average width of the medullary cavity between bone trabeculae, reflecting the morphology and structure of bone trabeculae. The greater the separation, the greater the distance between the bone trabeculae and risk of developing osteoporosis; (vi) The structure model index (SMI) defines the degree of plate-like and rod-like bone trabeculae. An SMI approaching 0 is indicative of more plate-like bone trabeculae, whereas an SMI approaching 3 is indicative of more rod-like bone trabeculae. The alterations in bone mass and microstructure are mainly caused by changes in the plate-like bone trabeculae, and (vii) The bone mineral density (BMD) ( $\text{g}/\text{cm}^3$ ) is an index reflecting alterations in bone mass and bone strength.

### Calculation of Spatial Percentages and Methods

In micro-CT analysis results, BV refers to the trabecular (or cortical) portion of the bone, and TV refers to the trabecular (or cortical) portion of the bone and cavity portion (without the osseous part). To define the total volume of screw paths and sclerosis around paths, all regions in each layer were divided, superimposed, and 3D-reconstructed to obtain the ratio of the TV part (screw paths and sclerosis region, collapsed region and relatively normal region) to the TV total (total femoral head volume). Subsequently, the results were used to determine the percentage of the three regions of interest to the total volume of the femoral head.

### Statistical Analyses

All data are expressed as means  $\pm$  standard deviations. SPSS (version 19.0, IBM Corp., Armonk, NY, USA) statistical software was used to analyze the data with a one-way analysis of variance. The level of significance was set at  $P < 0.05$ .

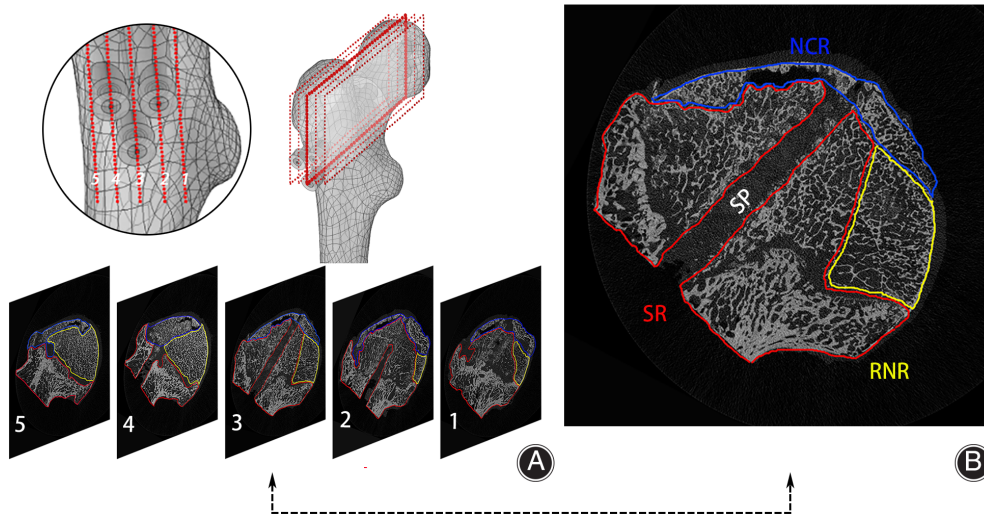


**Fig. 2** Micro-computed tomography analysis of a femoral head necrosis specimen 5 years after internal fixation for femoral neck fracture. (A) Five typical slices. Scanning along the direction of the implant placement for femoral neck fracture with a 20- $\mu$ m layer; approximately 1500 scans per femoral head were taken. (B) Schematic diagram the delineating the region of interest in each layer. The central slice of the middle screw path is used as an example, and is divided into the sclerosis region (SR; red), screw path (SP), relatively normal region (RNR; yellow) and necrotic collapsed region (NCR; blue).

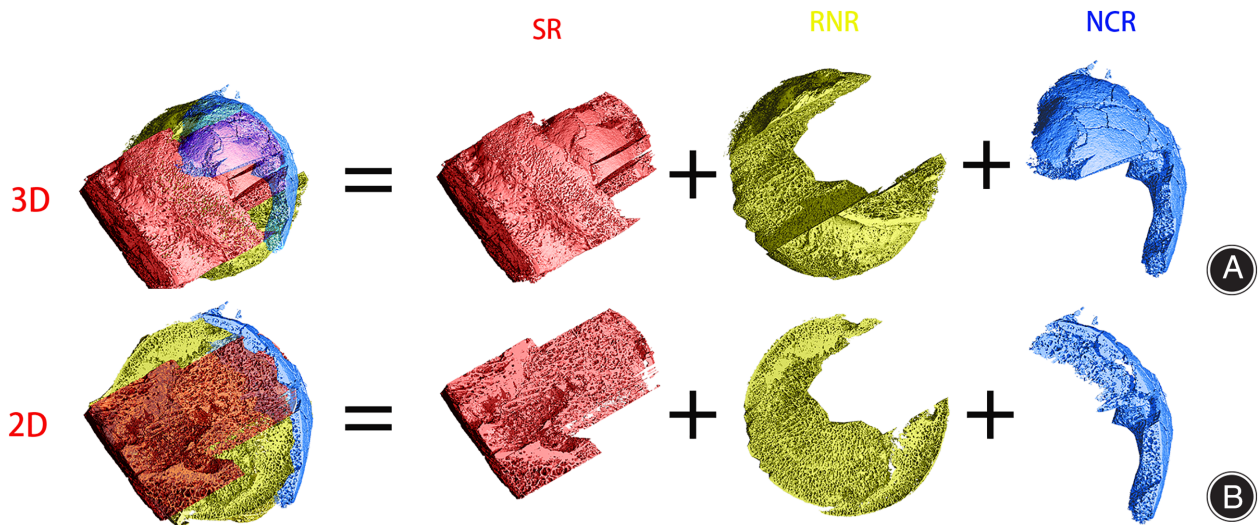


**Fig. 3** Computed tomographic images showing the region of interest in the N-layer that were selected and reconstructed to obtain bone trabecular parameters. (A) Two-dimensional and (B) three-dimensional images of the whole femoral head with each region of interest: sclerotic region (SR, red), relatively normal region (RNR, yellow), and necrotic collapsed region (NCR, blue).

## Results

### Results of 3D Analysis of Bone Trabeculae in Various Regions of the Femoral Head

#### Bone Volume Fraction (BV/TV)

Compared with those in the control group, the BV/TV ( $0.1248 \pm 0.0390$ ), total femoral head BV/TV ( $0.2448 \pm 0.0586$ ), sclerotic region around the screws BV/TV ( $0.3180 \pm 0.0617$ ), relatively normal region BV/TV ( $0.2162 \pm 0.0642$ ), and collapsed

region BV/TV ( $0.2222 \pm 0.0684$ ) in the experimental group were significantly higher ( $F = 5.374$ ,  $P < 0.05$ ). In the experimental group, the BV/TV was significantly higher in the sclerotic region around the screws than in the relatively normal and collapsed regions ( $P < 0.05$ ; as shown in Fig. 4A).

#### Trabecular Number (Tb.N)

The Tb.N was significantly higher in the sclerotic region around the screws ( $1.3533 \pm 0.2760$ )/mm in the

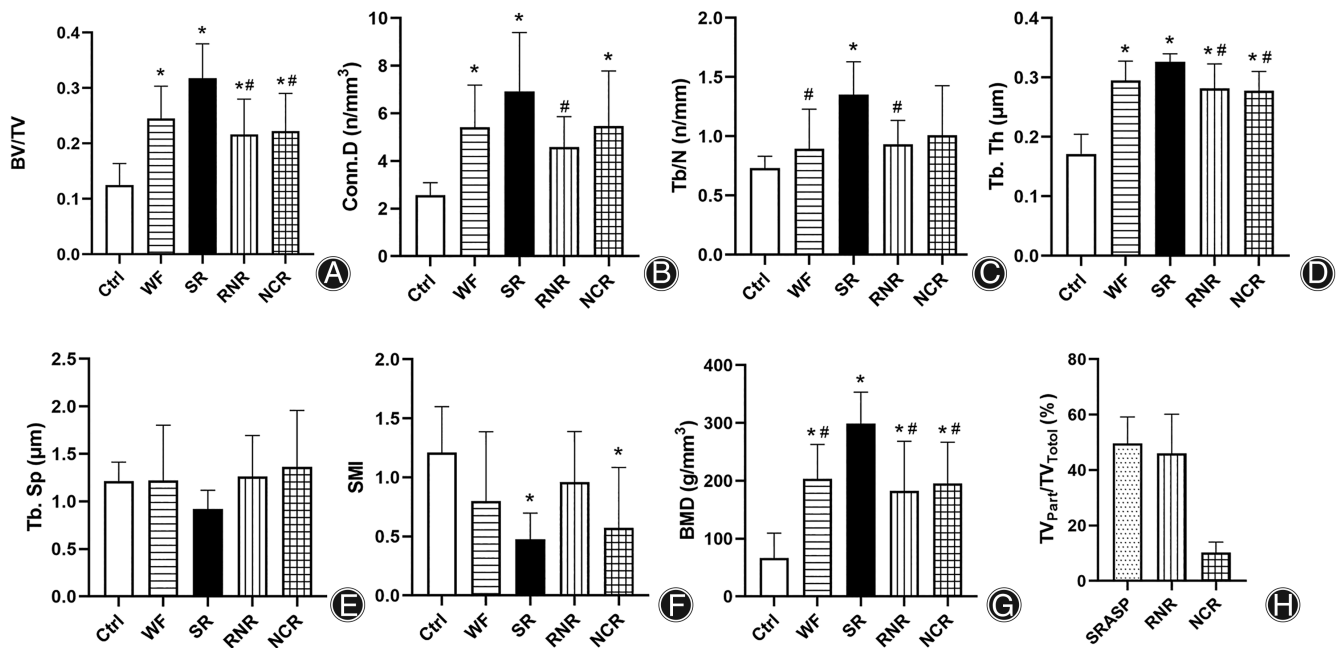


**Fig. 4** Micro-computed tomography results. Comparison of the (A) bone volume fraction (BV/TV), (B) connection density (Conn.D), (C) number of bone trabeculae (Tb.N), (D) thickness of bone trabeculae (Tb.Th), (E) separation of bone trabeculae (Tb.Sp), (F) structural model index (SMI), (G) bone mineral density (BMD), and (H) TVpart/TVwhole for each region of interest between the control and experimental groups. The experimental group specimen included the following regions: whole femur (WF), sclerotic region (SR), relatively normal region (RNR), necrotic collapsed region (NCR), sclerotic region, and screw path (SRASP). \* indicates a statistically significant difference compared with the control group ( $P < 0.05$ ). # indicates a statistically significant difference compared with the sclerotic region around the screw paths in the experimental group ( $P < 0.05$ ).

experimental group than in that in the control group ( $0.7314 \pm 0.0990$ )/mm. In the experimental group, the Tb.N was significantly higher ( $F = 2.852$ ,  $P < 0.05$ ) in the sclerotic region around the screws than in the overall femoral head ( $0.8914 \pm 0.3343$ )/mm and relatively normal region ( $0.9333 \pm 0.2011$ )/mm (Fig. 4B).

#### Connectivity Density (Conn.D.)

The Conn.D in the control group ( $2.5708 \pm 0.5187$ )/mm<sup>3</sup> was significantly higher ( $P < 0.05$ ) than the Conn.D in the entire femoral head ( $5.4131 \pm 1.773$ )/mm<sup>3</sup>, sclerotic region around the screws ( $6.9261 \pm 2.4715$ )/mm<sup>3</sup>, and collapsed region ( $5.4741 \pm 2.3024$ )/mm<sup>3</sup> in the experimental group. In the experimental group, the Conn.D was significantly higher in the sclerotic region around the screws than in the relatively normal region ( $F = 2.801$ ,  $P < 0.05$ ) (Fig. 4C).

#### Trabecular Thickness (Tb.Th)

In the experimental group, the Tb.Th was significantly higher in the following regions: entire femoral head ( $0.2952 \pm 0.0322$  μm), sclerotic region around the screws ( $0.3262 \pm 0.0136$  μm), relatively normal region ( $0.2817 \pm 0.0410$  μm), and collapsed region ( $0.2775 \pm 0.0326$  μm), than in the control group ( $0.1713 \pm 0.0333$  μm). In the experimental group, the Tb.Th was significantly higher in the sclerotic region around

the screws than that in the relatively normal and collapsed regions ( $F = 12.380$ ,  $P < 0.05$ ) (Figure 4D).

#### Trabecular Separation (Tb.Sp)

The Tb.Sp was slightly lower in the sclerotic region around the screws ( $0.9194 \pm 0.1980$  μm) than in the entire femoral head ( $1.2206 \pm 0.5823$  μm), relatively normal region ( $1.2605 \pm 0.4333$  μm), and collapsed region ( $1.3612 \pm 0.5965$  μm) in the experimental and control groups ( $1.2121 \pm 0.2025$  μm), although the difference was not statistically significant ( $F = 0.764$ ,  $P = 0.112$ ) (Fig. 4E).

#### Structure Model Index (SMI)

The SMI was significantly lower in the sclerotic region ( $0.4766 \pm 0.2200$ ) and collapsed region ( $0.5749 \pm 0.5085$ ) in the experimental group than in the control group ( $1.2115 \pm 0.3872$ ) ( $F = 2.016$ ,  $P < 0.05$ ). There was no statistically significant difference in the SMI between the entire femoral head ( $0.9649 \pm 0.4770$ ) and relatively normal region ( $0.9606 \pm 0.4292$ ) in the experimental group compared with that in the control group (Fig. 4F). The results showed that, compared with the bone trabeculae in the control group, the bone tissue in the sclerotic region around the screws and collapsed region in the experimental group was dominated by plate-like bone trabeculae.

### *Bone Mineral Density (BMD)*

The BMD was significantly higher ( $F = 6.347$ ,  $P < 0.05$ ) in the entire femoral head ( $203.4379 \pm 59.2638 \text{ g/cm}^3$ ), sclerotic region around the screws ( $298.9241 \pm 54.2029 \text{ g/cm}^3$ ), relatively normal region ( $182.5022 \pm 86.0429 \text{ g/cm}^3$ ), and collapsed region ( $195.0153 \pm 71.8509 \text{ g/cm}^3$ ) in the experimental group than in the control group ( $66.5181 \pm 43.0380 \text{ g/cm}^3$ ). In the experimental group, the BMD was significantly higher in the sclerotic region around the screws than in the entire femoral head and relatively normal and collapsed regions ( $P < 0.05$ ) (Fig. 4G).

### *Spatial Percentages of Different Regions of Femoral Head Necrosis after Surgery for Femoral Neck Fracture*

The results of the 3D reconstruction analysis showed that the volume ratio of the screw paths and sclerosis around the paths to the entire femoral head was  $0.4964 \pm 0.0950$ , the volume ratio of the relatively normal region to the entire femoral head was  $0.4599 \pm 0.1416$ , and the volume ratio of the collapsed region to the entire femoral head was  $0.1026 \pm 0.0379$  (Fig. 4H).

## Discussion

### *Micro-CT Analysis of Various Regions of the Femoral Head Trabeculae*

Healing of femoral neck fractures is a dynamic process of continuous remodeling of bone trabeculae, regulated *via* the mechanical load. The mechanical load in the early stage promotes the growth of bone trabeculae, which gradually tends to be balanced and maintains a certain mechanical performance.<sup>11</sup> However, when the mechanical load exceeds the bearing capacity, bone trabecular deformation and fracture will occur.<sup>16</sup> Femoral neck fractures change the anteversion of the femoral neck and disrupt the balance between structure and function,<sup>17</sup> which results in remodeling of the trabecular microstructure owing to the concentration of stress within the femoral head. If the remodeled structure cannot be used in the new compressive stress and other biomechanical environments, the bone trabeculae will degenerate, absorb, and collapse.<sup>18</sup> Furthermore, the surrounding vessels will become malformed and obstructed, leading to the development of femoral head necrosis. Micro-CT uses an X-ray source to emit X-rays that penetrate the sample from different angles using attenuation characteristics of its absorption to the image on the X-ray detector. Finally, the micro-CT reconstruction algorithm is used to reconstruct the 3D sample image. In contrast to medical CT, micro-CT can reach micron-level spatial resolution.<sup>19</sup> Wang *et al.*<sup>20</sup> used techniques involving the dissection-sensitive regions of the femoral head to analyze the spatial structure of the necrotic femoral head. In this study, non-invasive scans of different spatial and tomographic ranges of the necrotic femoral head samples after surgery for femoral neck fracture were performed using micro-CT. Holistic and local regions were combined, and the regions of interest underwent 2D division

and 3D reconstruction for quantitative analysis of the bone tissue metrology and spatial ratio in each region of the femoral head.

### *Mechanisms of Sclerotic Trabeculae Leading to Femoral Head Necrosis*

An increasing number of scholars emphasize that biomechanical factors play a significant role in the process of necrosis, while insufficient blood supply is found not to explain the mechanism of necrosis. The necrosis could also be observed in areas with an adequate blood supply. In fact, the stress concentration region of the femoral head in daily life is the region of femoral head necrosis and collapse.<sup>21</sup> Evidence indicates that compressive, tensile, and shear stresses to which the femoral neck is subjected are mainly concentrated around the implants after surgery.<sup>11,12</sup> Wang *et al.*<sup>10</sup> concluded that increase in stress loading leads to alterations in bone mass and microstructure, resulting in increased BV/TV, Tb.N, and Tb.Th of the bone tissue, without any significant influence on the microstructure of the rod-like bone trabeculae. In this study, micro-CT bone histomorphometry was performed for the detection of femoral head necrosis after surgery for femoral neck fracture. This demonstrated reduced SMI in the sclerotic region around the screws, which indicated that the bone trabecular structure around the implants was mostly plate-like, and the region had a significant increase in the BV/TV, Tb.Th, Conn.D, Tb.N, and BMD. These findings suggested that following long-term retention of implants, a large amount of sclerotic plate-like bone is formed around the implant after femoral neck fracture in middle age, and bone mass and BMD increase significantly. This adaptive sclerotic structure is probably formed to absorb the stress concentration around the screw paths, and the plate-like bone possesses an advantage for loading stress. Stress induction leads to the formation of a bone absorption region and is the initial factor for femoral head collapse and necrosis. Reduced tissue strength of the bone absorption region and restricted load transfer will lead to concentrated stress around the screw paths, further promoting stress-induced bone absorption and constantly expanding the formation of the sclerotic bone.<sup>22</sup>

### *Effect of Stress on the Femoral Head*

The normal femoral head mainly comprises spongy bone trabeculae with some elasticity.<sup>22</sup> The macro-Young's modulus and yield stress of bone tissue are significantly related to the bone volume fraction, which is correlated with the quantification of bone mass.<sup>15</sup> Our study showed that the BV/TV varied from region to region after internal fixation surgery for femoral neck fractures. In addition, the elasticity of each component against stress effects varied when the femoral head is subjected to external stresses, with the screw paths and sclerotic bone around the paths accounting for approximately 50% of the entire femoral head volume. Our study also showed that the BV/TV, Tb.Th, SMI, and BMD varied in the entire necrotic femoral head when compared with

those in the control group. This may be related to alterations in the trabecular structure and elastic function of the necrotic femoral head owing to the formation of plate-like sclerotic bone around the screw paths. It has been shown that bone trabeculae can be redistributed after surgery for femoral neck fracture to adapt to altered external stresses, and bone trabeculae are reconstructed in the same direction of alignment as the stress transfer. Normally, the stressed cortical and cancellous bone tissues transmit stress to the trochanter, where the greatest femoral trabecular stress is concentrated.<sup>23</sup>

Based on our results, it appears that most of the trabeculae around the internal fixation transformed into plates and the trabecular structure was disrupted, leading to necrosis, reconstruction of the cancellous bone around the screw, and eventually to the formation of sclerotic bone. Additionally, excessive deformation, which leads to microfractures and trabecular stiffness<sup>24</sup> can be accompanied by multiple repetitions of the ultimate stress loading on the femoral head. Retention of the implant results in the long-term concentration of stress on the femoral head, which may be an

underlying mechanism by which the femoral head can become necrotic despite a well-healed femoral neck fracture.

### Conclusion

The long-term preservation of implants is accompanied by the formation of a mass of sclerotic bone with a dense structure around the implants after internal fixation for femoral neck fracture. In addition, the screw paths and sclerotic bone account for approximately 50% of the entire femoral head. Implants and sclerotic bone may further undermine the mechanical and elastic structure of the femoral head. Our hypothesis that the long-term retention of internal fixation after femoral neck fracture leads to tissue sclerosis around the screw paths and osteogenic vascularization obstacles was verified.

### Limitations

In this study, only the overall structure of specimens approximately 3–6 years after femoral neck fracture was analyzed, and an analysis of the cancellous bone structure at different time points will also be required in the future.

## References

- Slobogean GP, Sprague SA, Scott T, Bhandari M. Complications following young femoral neck fractures. *Injury*. 2015;46:484–91.
- Tian FM, Zhang L, Zhao HY, Liang CY, Zhang N, Song HP. An increase in the incidence of hip fractures in Tangshan, China. *Osteoporos Int*. 2014;25:1321–5.
- Yang JJ, Lin LC, Chao KH, Chuang SY, Wu CC, Yeh TT, et al. Risk factors for nonunion in patients with intracapsular femoral neck fractures treated with three cannulated screws placed in either a triangle or an inverted triangle configuration. *J Bone Joint Surg Am*. 2013;95:61–9.
- Panteli M, Rodham P, Giannoudis PV. Biomechanical rationale for implant choices in femoral neck fracture fixation in the non-elderly. *Injury*. 2015;46:445–52.
- Large TM, Adams MR, Loeffler BJ, Gardner MJ. Posttraumatic avascular necrosis after proximal femur, proximal humerus, talar neck, and scaphoid fractures. *J Am Acad Orthop Surg*. 2019;27:794–805.
- Bhandari M, Swiontkowski M. Management of acute hip fracture. *N Engl J Med*. 2017;377:2053–62.
- Stockton DJ, O'Hara LM, O'Hara NN, Lefavre KA, O'Brien PJ, Slobogean GP. High rate of reoperation and conversion to total hip arthroplasty after internal fixation of young femoral neck fractures: a population-based study of 796 patients. *Acta Orthop*. 2019;90:21–5.
- Patterson JT, Ishii K, Tornetta P 3rd, Leighton RK, Friess DM, Jones CB, et al. Open reduction is associated with greater hazard of early reoperation after internal fixation of displaced femoral neck fractures in adults 18–65 years. *J Orthop Trauma*. 2020;34:294–301.
- Nyholm AM, Palm H, Sandholdt H, Troelsen A, Gromov K, DFKB COLLABORATORS. Risk of reoperation within 12 months following osteosynthesis of a displaced femoral neck fracture is linked mainly to initial fracture displacement while risk of death may be linked to bone quality: a cohort study from Danish Fracture Database. *Acta Orthop*. 2020;91:1–75.
- Wang H, Ji B, Liu XS, Guo XE, Huang Y, Hwang KC. Analysis of microstructural and mechanical alterations of trabecular bone in a simulated three-dimensional remodeling process. *J Biomech*. 2012;45:2417–25.
- Lambers FM, Koch K, Kuhn G, Ruffoni D, Weigt C, Schulte FA, et al. Trabecular bone adapts to long-term cyclic loading by increasing stiffness and normalization of dynamic morphometric rates. *Bone*. 2013;55:325–34.
- Wang Y, Ma JX, Yin T, Han Z, Cui SS, Liu ZP, et al. Correlation between reduction quality of femoral neck fracture and femoral head necrosis based on biomechanics. *Orthop Surg*. 2019;11:318–24.
- Zhou X, Yang YF, Niu WJ, Wei XC, Duan WP. Relationship between internal fixation removal and femoral head necrosis after femoral neck fracture in young and middle-aged patients: a meta-analysis. *Zhongguo Zu Zhi Gong Cheng Yan Jiu*. 2018;22:5724–4729.
- Zhang C, Zhang Y, Yu B, Zhang W, Sun H. Progress in treatment of femoral neck fracture in young adults. *Zhonghua Chuangshang Guke Zazhi*. 2018;20:921–8.
- Rieger R, Auregan JC, Hoc T. Micro-finite-element method to assess elastic properties of trabecular bone at micro- and macroscopic level. *Morphologie*. 2018;102:12–20.
- Zwahlen A, Christen D, Ruffoni D, Schneider P, Schmölz W, Müller R. Inverse finite element modeling for characterization of local elastic properties in image-guided failure assessment of human trabecular bone. *J Biomech Eng*. 2015;137:011012. <https://doi.org/10.1115/1.4028991>.
- Mourad C, Galant C, Wacheul E, Kirchgessner T, Michoux N, Vande BB. Topology of microfractures in osteonecrotic femoral heads at  $\mu$ CT and histology. *Bone*. 2020;141:115623.
- Kamal D, Alexandru DO, Kamal C, Streba CK, Grecu D, Mogoantă L. Macroscopic and microscopic findings in avascular necrosis of the femoral head. *Rom J Morphol Embryol*. 2012;53:557–61.
- Filippou V, Tsoumpas C. Recent advances on the development of phantoms using 3D printing for imaging with CT, MRI, PET, SPECT, and ultrasound. *Med Phys*. 2018;45:e740–60. <https://doi.org/10.1002/mp.13058>.
- Wang C, Wang X, Xu X, Yuan XL, Gou WL, Wang AY, et al. Bone microstructure and regional distribution of osteoblast and osteoclast activity in the osteonecrotic femoral head. *PLoS One*. 2014;9:e96361. <https://doi.org/10.1371/journal.pone.0096361>.
- Goda I, Assidi M, Ganghoffer J. Cosserat 3D anisotropic models of trabecular bone from the homogenisation of the trabecular structure. *Comput Methods Biomech Biomed Eng*. 2012;15:288–90.
- Ting BL, Heng M, Vrahas MS, Rodriguez EK, Harris MB, Weaver MJ. Is disuse osteopenia a favorable prognostic sign after femoral neck fracture? *J Orthop Trauma*. 2016;30:496–502.
- Carter D, Orr T, Fyhrie D. Relationships between loading history and femoral cancellous bone architecture. *J Biomech*. 1989;22:231–44.
- Martelli S, Perilli E. Time-elapsd synchrotron-light microstructural imaging of femoral neck fracture. *J Mech Behav Biomed Mater*. 2018;84:265–72.